Chapter 2

2.1 Introduction

Nanostructures of TMOs are synthesized using several established routes such as precipitation, co-precipitation, high energy ball milling, inert gas condensation, plasma deposition, reverse micelle technique, citrate precursor technique, micro-emulsion, hydrothermal reaction, sol–gel technique, polymer pyrolysis, liquid mix technique, etc. Every synthesis technique possesses a few advantages and disadvantages from technological and industrial point of view. The selection of an appropriate method to prepare versatile TMOs with different shape and size should be done cautiously. A synthesis route that is facile, rapid, inexpensive and capable of mass-production is sought for preparation of specific nanostructured metal oxides showing relevant and desired physical as well as chemical properties. In this chapter, we briefly summarize the synthesis method and deposition technique employed for the preparation of pure and rare earth doped HfO_2 powders and thin films, respectively. Afterwards, a concise overview of different characterization techniques utilized for studying the samples are discussed.

2.2 Powder Synthesis Method

In this work, HfO_2 powders were prepared through a simple Pechini type sol-gel technique. The flow chart of synthesis is shown in **figure 2.1**. For pure HfO_2 powders, the stoichiometric amount of hafnium chloride ($HfCl_4$, 99.9%, Alfa Aesar) was mixed with 2M citric acid ($C_6H_8O_7$) solution under constant stirring using a Teflon coated magnetic bead. Dy and/or Sm doped HfO_2 powders with varying concentration were produced by addition

of appropriate amounts of dysprosium nitrate ($Dy(NO_3)_3$, 99.9%, Sigma Aldrich) and samarium nitrate ($Sm(NO_3)_3$, 99.9%, Alfa Aesar) to previous solution mixture. Thereafter,

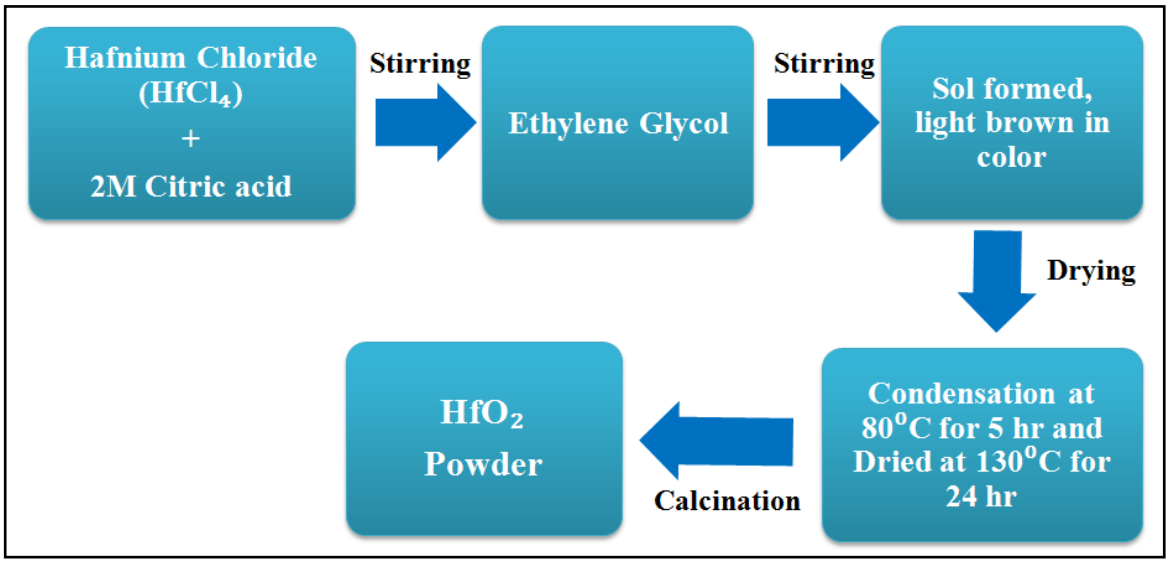

Figure 2.1 *Process flow of Sol-gel method for the synthesis of pure HfO_2 and rare earth doped HfO_2 powders.*

we obtained a clear solution ensuring complete dissolution of different precursors. A clear sol was formed after mixing the ethylene glycol (EG) ($C_2H_6O_2$) into the prepared solution leading to polymerization of sol. After heating the sol at 80 ^oC for 5 h to complete the condensation process, the sol was dried at 130 ^oC for 24 h in order to obtain the precursor resin. The dried out product was then pulverized in an agate mortar and pestle to obtain fine powder. Due to the presence of organic impurities, the prepared fine powder was slightly brown in color. Finally, the synthesized powders were calcined at different temperatures in air for 5 h to obtain pure HfO_2 and Dy and/or Sm doped HfO_2 which were white in color.

2.3 Thin Film Deposition

In the present thesis work, we have utilized the electron beam evaporation (EBE) technique to prepare HfO_2 thin films. EBE technique is a high vacuum based method peculiarly employed for thin film deposition of several metal oxides. The EBE deposition system requires the base pressure of ~10^{-6} mbar in deposition chamber, facilitating the route for generated electrons from the electron gun to target material for evaporation. The pure target materials are available as pellet, ingot or rod. The upgraded EBE deposition systems working on an arc suppression system can also work at even ultrahigh vacuum levels (10^{-9} mbar). There exists the possibility of deployment of different kinds and number of the evaporation materials as well as electron guns simultaneously in a single system. The power of electron guns may vary from a few tens to hundreds of kW.

Figure 2.2 depicts the schematic diagram of a standard EBE deposition system. The strong beam of energetic electrons can be produced by different techniques like thermionic emission and field emission including anodic arc method. Under the presence of appropriate magnetic field, the electron beam is accelerated to a high kinetic energy which is then bend towards the target material for deposition. When this electron beam strikes the material, the electron quickly loses its kinetic energy transferring into other forms of energy after interacting with target material. A sufficient thermal energy produced in such a way that it heats and consequently melts or sublimates the target material. After attaining attaining the suitable temperature at desired vacuum level, a vapor plume appears from the melted or sublimated target material. This vapor plume of target material is coated onto the substrates. The accelerating voltage can be used from 3 – 40 kV. After optimizing this voltage (20 – 25 kV) with suitable beam current, most of the kinetic energy of electrons is

transformed into equivalent thermal energy. The incident energy of electron is partially lost for generating X-rays and other secondary electron emissions.

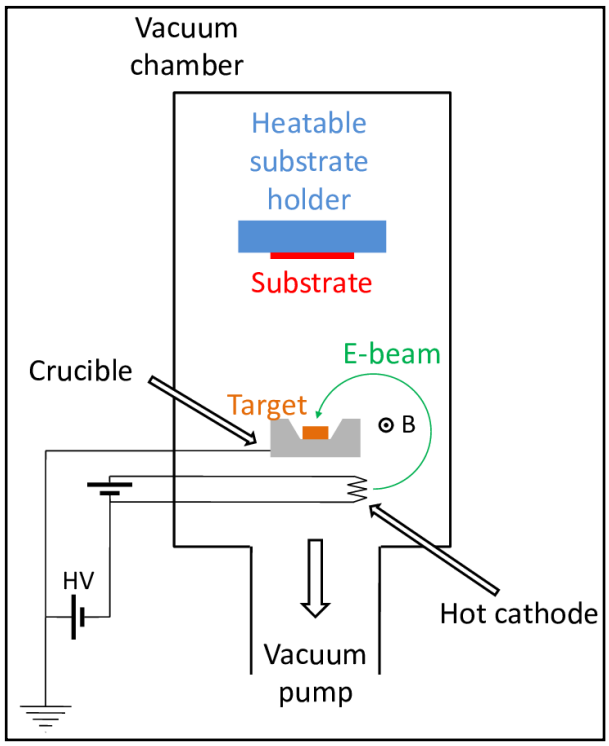

Figure 2.2 *A schematic representation of electron beam evaporation (EBE) deposition system. (the direction of magnetic field (B) is out of the page).*

In particular, EBE deposition system can be built using following configurations:

1. Electromagnetic alignment

2. Electromagnetic focusing

3. Pendant drop configuration

While the target material in its ingot form is usually used for electromagnetic alignment and electromagnetic focusing, a rod shaped target evaporation material is

employed in the pendant drop configuration. The crucible or hearth made of copper metal is used for mounting the ingot shaped target material. However, the target in rod shape is placed at one end in the socket. Due to production of excess heat after incidence of electron beam, the holders of target material like crucible and socket is cooled continuously. In general, continuous circulation of cool water is utilized for same. EBE deposition system can provide relatively large rate of evaporation in the order of 10^{-2} g.cm^{-2}.s.

EBE deposition system is capable of evaporating materials with high melting point such as refractories e.g. titanium carbide and borides, including zirconium boride without showing decomposition of the material. The evaporated target material is directly deposited onto different substrates. There are some refractory metal oxides and carbides which fragment in the process of evaporation leading to a off-stoichiometry of the target material. This is generally observed in case of alumina. When the electron beam strikes alumina, it can possibly dissociates and form aluminum, AlO_3 and Al_2O. Such decomposition can also occur in silicon carbide and tungsten carbide materials producing elements with dissimilar volatilities. However, most of the target materials like HfO_2 having very high melting point (>2500 ^oC) are easily deposited using EBE system without undergoing any decomposition. In addition, EBE deposition technique is also very useful for depositing different metals such as silver, copper, aluminum, and tungsten etc. This deposition technique offers substantially wide range for rate of deposition from 1 nm per minute to very high rates of a few μm per minute. The structural and morphological properties of deposited films can be controlled during deposition with great utilization efficiency of the material.

HfO_2, Sm and Dy doped HfO_2 films were deposited onto cleaned p^{++}-Si substrates through EBE deposition technique using individual pure pellet targets of HfO_2, Sm and Dy

doped HfO_2. During the film deposition, the substrate temperature was kept at room temperature and the vacuum chamber base pressure was maintained at ~6 X 10^{-6} mbar. After deposition, the films were annealed at 550 ^{o}C for 60 min in air followed by subsequent characterizations.

2.4 Device Fabrication for RRAM

2.4.1 Cleaning of p^{++}-Si

Prior to deposition, first, highly doped p-type silicon substrate (p^{++}-Si) of size 1 X 1 cm^2 is dipped into strong Piranha solution (H_2SO_4 : H_2O_2 = 7 : 1) for 3 min to etch the silicon surface for removal of unwanted native oxide and subsequently washed several times with DI water. After this treatment, the silicon substrates are successively cleaned using acetone and isopropanol for 5 min each with the help of ultrasonic bath followed by drying process via passing dry air. The thoroughly cleaned p^{++}-Si substrates are then used for deposition of thin films.

2.4.2 Fabrication of Metal-Insulator-Metal (MIM) Test Structures

HfO_2, Sm and Dy doped HfO_2 films are deposited onto the thoroughly cleaned p^{++}-Si substrates. In order to perform electrical characterization, MIM test structures consisting of Al/HfO_2/ p^{++}-Si are fabricated. p^{++}-Si acts as the bottom electrode and aluminum is used for the top electrode material. Using metal shadow mask, the circular Al top electrode with diameter of 500 μm is deposited on the top of HfO_2/ p^{++}-Si through thermal evaporator under the chamber pressure of ~10^{-6} mbar. The schematic of MIM test structure is shown in **figure 2.3**.

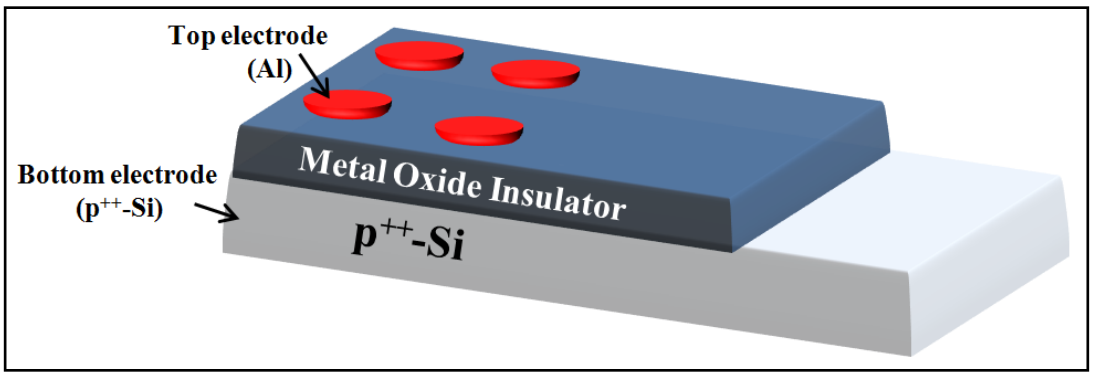

Figure 2.3 *The schematic diagram of metal-insulator-metal (MIM) test structure.*

2.5 Characterization Techniques

Pure, Dy and/or Sm doped HfO_2 nanostructured samples have been systematically characterized by employing appropriate techniques to analyze structure, magnetic, optical and electrical properties. The different characterization techniques utilized in the present thesis work are briefly discussed below.

2.5.1 X-ray Diffraction (XRD) for Powder Samples

XRD is the most widely used technique primarily employed to determine the crystal structure of a particular material. A non-destructive technique like XRD is peculiarly utilized as the preliminary characterization tool for extracting structure related information such as phase formation, crystallite size and lattice strain etc. In this technique, an electromagnetic wave having the wavelength of ~1 Å is diffracted from the crystal lattice planes oriented in different direction in crystal. This is achieved due to comparable order of magnitude of the X-ray wavelength and crystal lattice. XRD essentially facilitates the identification of different crystalline structure present in the material. The basic principle of XRD is based on the Bragg's law which states that the incident X-rays are diffracted from a

set of equally spaced lattice planes in the crystal that interfere constructively. These diffracted X-rays interfere constructively if the path difference between them is an integral multiple of the X-ray wavelength. This is given by Bragg and known as Bragg's law which is expressed as, $2d_{hkl}\,Sin\theta = n\lambda$ where, d_{hkl} is called as the interplanar distance (*hkl* are Miller indices), θ is the Bragg's angle, n is an integer indicating order of diffraction (n = 1 for XRD) and λ is X-ray wavelength. An illustration of the Bragg's law is demonstrated in **figure 2.4**.

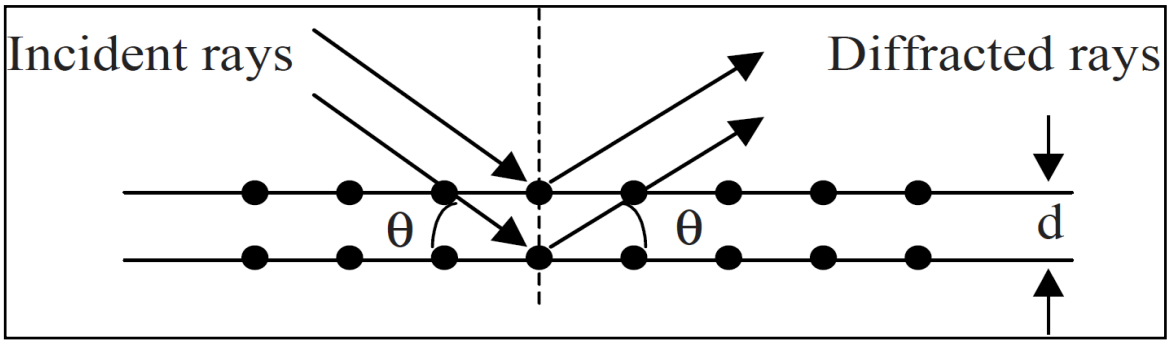

Figure 2.4 *A representation of the incident X-rays and their diffraction from equidistant lattice planes.*

Due to the constructive interference satisfying the Bragg's law, the diffraction pattern exhibits high intense peaks at certain scattering angles. In general, while the crystals possessing low symmetry structure e.g. monoclinic reveal several diffraction peaks because of numerous lattice planes, a few number of diffraction peaks are observed in case of high symmetry structures such as cubic and tetragonal containing certain lattice planes. The nature of diffraction peaks and their intensities is also dependent upon the size and shape of particles in the crystal.

In practice, an accelerated electron beam of required energy is directed towards the copper metal target which eventually produces X-rays. The collimated characteristic X-rays (K_α) having wavelength of 1.54 Å are utilized to characterize the material. Most of the diffractometer works on the para-focusing (or Bragg-Brentano) configuration. This geometry is the most common and well suited for different materials. The samples with flat surfaces are easily diffracted for collection of data using the detector. The detector essentially converts diffracted beam into a count rate. The detector and sample can rotate by an angle 2θ and θ, respectively. Finally, the plot consisting of a series of diffraction peaks as a function of diffraction angle is realized that can be used for analysis of the crystal structure. Usually, the XRD patterns are recorded in the range of $2\theta = 10 – 120^o$.

In this work, XRD patterns were obtained on a Rigaku Miniflex X-ray diffractometer using Cu Kα (λ = 1.54 Å) operating in Bragg-Brentano geometry. The indexing of XRD patterns were identified using Joint Committee on Powder Diffraction Standards data (JCPDS). Using Le-Bail profile fitting of FULLPROF program, the different structural parameters like lattice constants and cell volume are extracted for synthesized samples. This fitting technique is based on matching the suitable generated intensities with experimental data to determine the particular crystal structure of a specific space group.

2.5.2 Grazing Incidence X-ray diffraction (GIXRD) for Thin Films

GIXRD works on the same principle of Bragg's law. While performing measurements of thin films, the XRD instrument used particularly for powder samples produces the high intensity diffraction peaks from the substrates resulting into weak signal from the thin film. Consequently, in such cases, the signal-to-noise ratio is very low

rendering poor information related to structure of the film. In contrast to Bragg-Brentano geometry, GIXRD uses the low incident angle near critical angle and the detector performs a 2θ scan. At a low and constant angle of incidence angle, X-ray beam does not penetrate into the thin film which increases the diffraction coming from films rather than the substrate. Here, we have used GIXRD from Rigaku SmartLab equipped with PhotonMax high-flux 9 kW X-ray source of rotating Cu anode producing Cu Kα (λ = 1.54 Å). It uses the high-energy-resolution 2D multidimensional semiconductor detector for 0D, 1D and 2D measurement modes. This instrument comes with a high-resolution θ/θ closed loop goniometer drive system with an available in-plane diffraction arm. The embedded Cross-Beam-Optics (CBO) allows automated switchable reflection and transmission optics. For all prepared thin film samples, GIXRD patterns are collected from 2θ = 20-80 ^{o} at a scan rate of 3^{o}/min.

2.5.3 X-ray reflectivity (XRR)

XRR is one of the versatile and potential surface sensitive technique used for the measurement of thickness of thin films including multilayers, surface along with interface roughness, surface density gradients and layer density etc. In this work, we have used Bruker D8 Advance diffractometer with X-ray source of wavelength 1.54 Å to estimate the thickness and film density using X-ray reflectivity (XRR) measurements. The experimental XRR patterns were then fitted with suitable stack models using Parratt software.

2.5.4 Electron Probe Micro Analysis (EPMA)

EMPA, a non-destructive technique is extensively used for elemental determination of samples in the form of a solid. In this technique, a highly collimated beam of energetic electrons having the typical energy of 5 – 30 keV excites the X-rays of specific element.

The obtained X-ray spectrum exhibits distinct features related to different elements constituting the sample. Both qualitative and quantitative analysis can be perceived utilizing the X-ray spectrum. revealing a specific wavelength or photon of definite energy. A comparison of relative intensities of different characteristic lines provide quantitative information of element concentration in the sample. In practice, EPMA includes other spectroscopic instrumentation like wavelength dispersive spectroscopy (WDS), energy dispersive spectroscopy (EDS), scanning electron microscopy (SEM) and back scattered electron (BSE) imaging. Therefore, it is capable of offering a facile detection of elemental composition. Due to the combination with WDS spectrometers which work on Bragg's law, this instrument is highly sensitive even to extremely low element concentration up to a few tens of ppm (parts per million) without compromising the accuracy of detection. With limited spatial resolution of ~1 mm, the spatial distributions are collected as line spectrum or 2D (two-dimensional) map.

Here, EPMA, CAMECA, SX Five has been employed as an efficient tool for facile detection and analysis related to distribution of constituting elements for investigating the composition of the synthesized samples. WDS spectra were recorded for elemental analysis. A focused electron beam obtained with 15 kV accelerating voltage having a beam current of 4 nA was used for analysis. TAP (thallium acid phthalate), PET (pentae´rythriol) and LLIF (long lithium fluoride) crystals were further used to record the spectra.

2.5.5 Transmission Electron Microscopy (TEM)

TEM is primarily used to examine the microstructure of the material. It also offers vital information related to morphology such as shape and size of the particles including their specific size distribution histograms (i.e. particle size with frequency of particles). A

variety of TEM instruments e.g. high resolution TEM (HRTEM), scanning TEM (STEM) and analytical TEM (ATEM) are employed for different investigations. The instrumentation of standard TEM includes: (i) an electron gun, (ii) the vacuum system, (iii) focusing electromagnetic lenses, (iv) the high voltage generator and (v) imaging electronic devices. The collimation of electron beam is achieved using the electromagnetic condenser lenses. This beam exhibits relatively lower wavelength rendering excellent resolution under 0.2 nm. The well focused beam of very high energy typically more than ~200 keV is incident onto the sample which scatter and partially transmitted towards the objective lens that is imaged upon the charge coupled device (CCD) camera. Apart from common imaging mode, TEM can produce a specific diffraction patterns.

This work utilizes an FEI make Tecnai G^2 20 Twin instrument for imaging, selected area electron diffraction (SAED) pattern and high resolution TEM. The size and shape of particles including particle size distribution histogram could be realized from micrographs and analyzed using ImageJ software. SAED patterns exhibit distinct and continuous concentric rings which are examined after estimating inverse of their radii and matching with interplanar spacing (*d*) calculated from XRD data. HRTEM imaging mode revealed lattice information at atomic scale. The distinct lattice planes in HRTEM are realized for estimation of *d* value corresponding to a specific crystal plane.

2.5.6 Scanning Electron Microscopy (SEM)

SEM finds substantial use in analyzing topography of the sample. It primarily images the texture of different surfaces. The incident electron beam onto the sample surface ionizes the atoms which can consequently emit the loosely bound electrons called as the secondary electrons. These secondary electrons exhibit relatively low energy in the

range of ~3 to 5 eV. Such electrons are capable of marking the position of the beam very precisely which contained information related to topography of the surface. The secondary electrons can be easily detected due to their low energy. A high contrast image is formed after scanning the beam onto a screen or computer monitor. With proper detection mode, remarkable contrast against topography can be achieved. SEM shows good spatial resolution of the order of 10 nm or better, thereby resolves most of the surface structures. Using different kinds of detectors, SEM can be used for extended implementation in cathodoluminescence (CL). We have utilized field emission, FE-SEM, Nova Nano-SEM of FEI make for recording images and energy dispersive spectra (EDS) of the specimen.

2.5.7 X-ray Photoelectron Spectroscopy (XPS)

XPS known as electron spectroscopy for chemical analysis (ESCA) examines the elements, oxidation state of the constituent element and valence band structure by probing the surface of specimen. Since, this is a surface sensitive technique, it provides essentially the relative composition on the surface only. XPS is based on the photoelectric effect i.e. the emission of electron following excitation of core level electrons by energetic X-ray photons of energy, hv. The kinetic energy (K.E.) of electrons emitted in such is expressed as follows:

$$\text{K.E.} = hv - \text{B.E.} - \phi \qquad (2.1)$$

where B.E. is the binding energy of an individual electron and ϕ is the work function. Explicitly, when the energy of X-ray photon is larger than the binding energy, the photoelectrons are emitted from the core levels. [Stickle et al. (1992)]. These photoelectrons can be identified by their respective kinetic energy. The XPS spectra are drawn between the frequency of emitted electrons as a function of their K.E. The B.E. of

different electronic state is calculated with respect to the Fermi energy level. For a certain photon energy, the K.E. distribution of the photoelectrons implies the energy distribution of electronic states. These photoelectrons are usually scattered from nearby electrons, plasmons and/or phonons which slow down energetic electron after partially losing their energy. Due to significant loss in energy, the photoexcited electrons do not pass through the specimen. This undesirable scattering of photoelectron results into unwanted secondary inelastic background intensity. Such scattering is more prominent within the low range of kinetic energy occurring because of strong electron-electron interaction. Although X-ray can penetrate upto large depths into specimen, only the photoelectrons originating from a depth of a few tens of angstrom can be detected due to high degree of scattering. After the collision or scattering, photoelectrons with sufficient kinetic energy surpass the work function barrier and reaches the detector.

In general, the scattering and collisions between emitted electrons is reduced when the chamber is evacuated to ultra high vacuum. This enhances the mean free path of the emitting electrons which easily reaches to the detector. The monoenergetic soft X-rays are more appropriate energy source for exciting the photoelectrons. A compatible electrostatic analyzer is used to analyze the excited photoelectrons. In this study, XPS measurements are performed on VSW and AMICUS make X-ray photoelectron spectrometer utilizing radiations of Al-Kα (1486.6 eV) and Mg-Kα (1253.6 eV), respectively. The sample preparation chamber is evacuated to ~10^{-8} Torr whereas the vacuum level of sample analysis chamber is maintained at ~10^{-9} Torr. The scanning is first carried out to collect the complete range of energy i.e. survey scan. Afterwards, for the precise elemental analysis and sample composition in our study, O 1*s*, Hf 4*f*, Sm 3*d* and Dy 4*d* core level spectra are

selectively recorded. All the recorded core level spectra were calibrated with respect to C 1*s* peak centered at ~284.8 eV. XPS spectra were deconvoluted using XPS 4.1 software.

2.5.8 Magnetic Measurements

Magnetic properties of the synthesized samples are investigated by means of field and temperature dependent magnetization measurements employing magnetic properties measurements system (MPMS3 of Quantum Design, USA). This instrument uses vibrating sample magnetometer (VSM) and the superconducting quantum interference device (SQUID) for the measurement of magnetic moment. This facility is avaiable at Central Instrument Facility (CIF), IIT (BHU), India. A concise overview of including the working principle of both VSM and SQUID is provided below.

i) Vibrating Sample Magnetometer (VSM)

VSM is capable of measuring the magnetic moment of the specimen maintaining excellent accuracy. DC magnetization measurements of samples are performed with VSM operating between temperature range of 2 - 400 K and magnetic field of ± 7 Tesla. In this magnetometer, the measurement of magnetic moment with high precision is achieved with induction method. This method essentially involves the measurement of voltage which induces in a set of detection coils when the magnetic moment changes slightly in the sample. In practice, the measurement of induced voltage at the detection coil can be performed by vibrating speciemen with constant frequency under a uniform magnetic field.

In a specimen, there exists numerous magnetic dipole. in the beginning, the specimen is fixed at the center of the detection coil. When it is displaced to a certain distance in time, *t*, the change in flux (ϕ) inducing a voltage given by $v = d\phi/dt$ which is measured in the detection coils. Usually, these detection coils are placed inside a solenoid

producing the magnetic field. The resulting moment in specimen is then measured with respect to applied magnetic field.

ii) SQUID Magnetometer

In order to measure minute magnetic moment in the specimen, SQUID is known to be the most suitable and sensitive technique. This device measures very small magnetic field utilizing the superconducting loops prenset in Josephson junction. Specifically, SQUID indirectly meausres the magnetic field of specimen. In general, when the specimen passes through superconducting detection coils connected with the SQUID via superconducting wires. This enables the flow of current from the detection coils to inductively coupled high quality sensors. The current from these coils is converted to equivalent voltage through SQUID. The whole assembly of instrumentation can be divied into following primary components: the main device i.e. SQUID, a magnetic flux transformer with appropriate detection coils, the superconducting magnetic coil, heat switches including suitable magnetic shielding configuration. Superconducting detection coils do not response to uniform and linear magnetic fields since the coils are set as second-order gradiometer having counter wound outer loops. When the local magnetic field changes, it produces a certain current in the detection coils. In practical situations, SQUID can response to every small change in the magnetic field. For this reason, the magnetic shielding is of utmost importance to prevent the sensor detecting stray fields arising from ambient or laboratory or the large magnetic fields originating from superconducting coil. The small area where magnetic field changes in detection coils, the heaters are used to remove the standing currents in the superconducting loops by raising them beyond their critical temperature. SQUID offers remarkable sensitivity of ~5 x 10^{-8} emu and frequency

range of 0.1 - 1 kHz. The measurement and removal of background ac phase shifts for each measurement is done through direct phase nulling technique. The rate of temperature change is 10 K/min from 300 to 10 K and then cool down very slowly from 10 to 2 K at 2 K/min.

2.5.9 Photoluminescence (PL) Measurements

PL spectroscopy is a nondestructive and widely used technique to study the electronic structure of different materials. Under irradiation of light, the electrons are transfterred to excited state after absorbing energy of the photon and while coming back to ground state, lose this energy in the form of emission or luminescence. The photoluminescence is the emission of certain wavlength of light when the sample is exposed to light. The emissions of light are realized in different ways i.e. spectrally, spatially and temporally. The optical excitation of electrons is termed as the transfer of energetic electron to definte allowed excited states. The relaxation of these electrons towards ground or lower energy states can either emit light through a radiative process or may not produce light which is known as the non radiative process. The emitted light exhibits energy equal to the difference between final (excited) and initial (ground state) energy levels of the participating electrons. For the PL spectroscopic measurements, laser light or xenon lamp is used as the excitation source with variable energy. The time dependent PL decay measures the respective rate of radiative recombination process. The nonradiative recombination centers are analyzed by the temperature dependent behavior of the PL intensity. PL technique is also very much useful for analyzing the purity, crystalline quality and concentration of impurity and/or defects present in the material. An excitation spectrum is obtained for a particular emission wavelength which is partly similar to an

absorption spectrum. At a certain wavelength known as the excitation wavelength, the specimen can produce the emission spectrum characteristic of the materials. For the fixed excitation and emission wavelength, the PL decay curves are recorded as a function of time.

PL spectrofluorometer measures and collects the spectra of fluorescence and phosphorence from the sample. During the fluorescence mode, the excitation and emission spectra are recorded for a range of wavelength. PL instrument can be modified with additional attachments for analyzing the emission behavior with time, temperature, concentration and polarization etc. A standard fluorescence spectrometers contains following main components shown in **figure 2.5**.

Illuminator source:- The illuminator is a continuous source of light obtained either by monochromatic laser or LED or broadband xenon lamp. The light originating from illuminator source is collimated through a set of elliptical mirrors along with lenses and delivered to the entrance slit of the excitation monochromator via optical fibers. The light source and excitation monochromator are separated using the window made of quartz. This is also used to release out the excess heating that may damage the light source.

Monochromators:- In practical PL instruments, there exists two different monochromators namely the excitation monochromator and emission monochromator. These monochromators offer high resolution for the complete wavelength range utilizing appropritate reflective optics by reducing spherical aberrations and re diffraction.

Gratings:- In the monochromator, the reflection grating is used to disperses the incident light occurring beacuse of the embedded vertical grooves and provides a good spectral resolution. The spectrum can be collected by a ruled blazed gratings with 1200

lines/mm(l/mm) blazed at 330 and 500 nm for excitation and emission monochromator, respectively. MgF_2 layer onto these gratings prevents the unwanted oxidation.

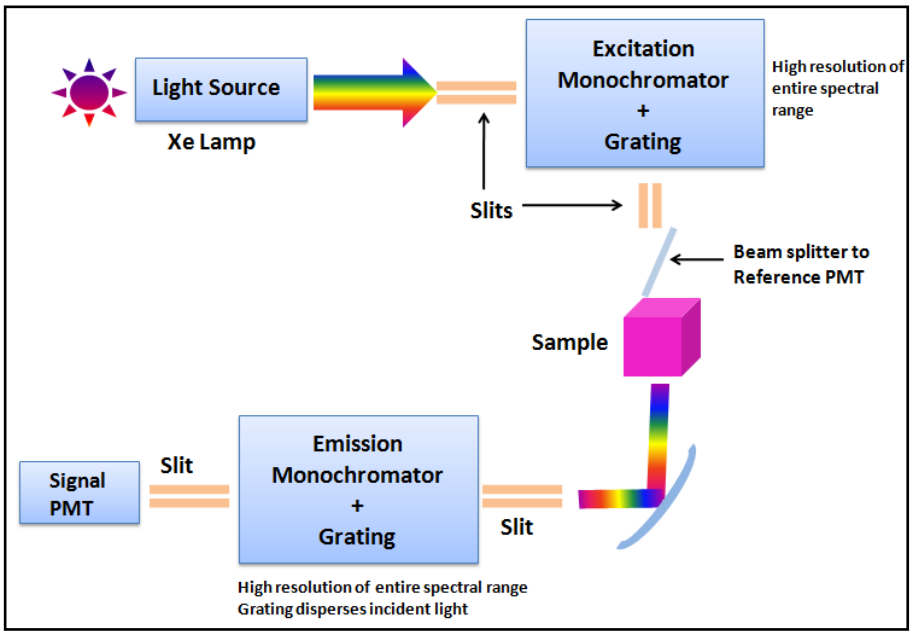

Figure 2.5 *A standard PL spectrofluorometer indicating different components used in the experimental setup.*

Slits:- Both the monochromators contain entrance and exit slits which can be controlled for required amount of light. At the excitation monochromator, slit width allows certain band of light to transfer towards the sample. The slit at emission monochromator can be adjusted for signal intensity at the detector. An appropriate slit width produces the maximum intensity maintaining a high resolution over the whole spectral range.

Detectors:- There are two types of detectors present in the spectrofluorometer i) reference detector and ii) signal detector. A reference detector is used for the light source in which wavelength correction and light source output with respect to time is monitored. This detector is kind of photomultiplier tube (PMT) placed infront of the sample. The fluorescence signal detector is also a PMT transferring the signal to the photon counting module. In present thesis work, the room temperature excitation, emission spectra along

with time resolved decay curves have been measured with a Horiba, Jobin Yvon, Fluorolog using the excitation source of a 450 W Xe arc lamp. The spectral resolution of the above spectrometer is 1 nm. The braod spectral range spans from 200-2000 nm for collecting excitation and emission spectra. Further, CIE (*Commission Internationale de l'Éclairage*) diagram has been used to characterize the hue and purity of different colors. In practice, CIE diagram drawn into two dimension (2D, *xy*) plot consists of chromaticity coordinates (*x, y, z*) and tristimulus values (X, Y, Z) expressed as following mathematical relations.

$$x = X/(X+Y+Z),\ y = Y/(X+Y+Z),\ z = Z/(X+Y+Z)$$

X, Y, Z represents primary colors red, green and blue which reconstruct hue and various combinations of colors with distinct wavelengths which are easily perceived by a standard observer. Within CIE 2D *xy* diagram, a horseshoe shape is formed for a wide range of wavelength spectrum (chromatic values) producing all available pure color chromaticity. For a given emission spectrum, *x,y* are calculated using dedicated software which provide a point position in CIE diagram indicating nature and purity of produced color.

2.5.10 Current-voltage (*I-V*) Measurements

The current-voltage (*I-V*) characteristics of MIM test structures (**figure 2.3**) are performed on the Keysight, USA make semiconductor parameter analyzer (Model No.: B1500A). *I-V* measurements are carried out after sweeping the applied DC bias voltage in a sequence of 0 V→ 4 V→ 0 V→ -5 V→ 0 V. The electrical contact of MIM was made using probe micromanipulator. During *I-V* measurements, the bottom electrode (p^{++}-Si) has been grounded and the bias voltage applied to the top electrode only. In order to avoid undesirable electrical breakdown of devices, the compliance current was fixed at 7 mA during the measurements.